In Vivo Medial and Lateral Tibial Loads during Dynamic and High Flexion Activities

Dong Zhao,[1] Scott A. Banks,[1,2,3] Darryl D. D'Lima,[4] Clifford W. Colwell Jr.,[4] Benjamin J. Fregly[1,2,3]

[1]Department of Mechanical & Aerospace Engineering, University of Florida, Gainesville, Florida

[2]Department of Orthopaedics and Rehabilitation, University of Florida, Gainesville, Florida

[3]Department of Biomedical Engineering, University of Florida, Gainesville, Florida

[4]Shiley Center for Orthopaedic Research & Education at Scripps Clinic, La Jolla, California

Received 14 February 2006; accepted 12 November 2006

Published online 8 February 2007 in Wiley InterScience (www.interscience.wiley.com). DOI 10.1002/jor.20362

ABSTRACT: Though asymmetric loading between the medial and lateral compartments of total knee replacements may contribute to implant loosening and failure, the in vivo contact force distribution during dynamic daily activities remains unknown. This study reports in vivo medial and lateral contact forces experienced by a well-aligned knee implant for a variety of activities. In vivo implant motion and total axial load data were collected from a single knee replacement patient performing treadmill gait (hands resting on handlebars), step up/down, lunge, and kneel activities. In vivo motion was measured using video fluoroscopy, while in vivo axial loads were collected simultaneously using an instrumented tibial component. An elastic foundation contact model employing linear and nonlinear polyethylene material properties was constructed to calculate medial and lateral contact forces based on the measured kinematics, total axial loads, and centers of pressure. For all activities, the predicted medial and lateral contact forces were insensitive to the selected material model. The percentage of medial to total contact force ranged from 18 to 60 for gait, 47 to 65 for step up/down, and 55 to 60 for kneel and lunge. At maximum load during the motion cycle, medial force was 1.2 BW for gait and 2.0 BW for step up/down, while the corresponding lateral forces were 1.0 and 1.5 BW, respectively. At mean load in the final static pose, medial force was 0.2 BW for kneel and 0.9 BW for lunge, with corresponding lateral forces of 0.1 and 0.7 BW, respectively. For this patient, a constant load split of 55% medial–45% lateral during loaded activity would be a reasonable approximation for these test conditions. © 2007 Orthopaedic Research Society. Published by Wiley Periodicals, Inc. J Orthop Res 25:593–602, 2007

Keywords: elastic foundation contact model; in vivo knee forces; total knee arthroplasty; instrumented knee implant

INTRODUCTION

Asymmetric loading between the medial and lateral compartments of the knee has been hypothesized to contribute to the development of knee osteoarthritis (OA).[1] In artificial knees, asymmetric forces exerted on the tibial insert may contribute to mechanical failure and implant loosening.[2] Ever since Morrison's[3] seminal work, modeling studies have predicted larger contact forces on the medial than on the lateral side of the knee during gait.[4–9] These studies have reported between 50 and 100% of the total contact force passing through the medial compartment, with the predicted medial-lateral load split varying considerably over the gait cycle.[5] While recent experimental studies have measured in vivo axial loads in the femur and tibia using telemetry,[10–12] none have been able to partition the total axial load into medial and lateral contact forces. Thus, the actual in vivo distribution of tibial contact forces during dynamic, weight-bearing activities remains unknown.

The lack of accurate in vivo medial and lateral contact force data is also problematic for predicting abrasive/adhesive wear in total knee replacements. Medial-lateral load split affects medial and lateral contact pressures, which in turn affect mild wear of the polyethylene tibial insert.[13] For lack of better data, researchers often offset the axial load 5 mm to the medial side when evaluating the wear performance of a new implant design using a knee simulator.[14] Though in vivo contact pressures have

Correspondence to: Benjamin J. Fregly (Telephone: 352-392-8157; Fax: 352-392-7303; E-mail: fregly@ufl.edu)

been predicted by computational models,[15,16] they too suffer from assumptions related to the unknown medial-lateral load split.

This study sought to determine in vivo medial and lateral tibial loads during gait, step up/down, kneel, and lunge activities for a single knee implant patient. Contact forces during each activity were found using a novel combination of experimental and computational techniques. The results provide insight into the in vivo loading conditions experienced by a well-aligned knee implant for a variety of activities.

METHODS

Data were collected from one patient (male, right knee, age 80 years, mass 68 kg) eight months after surgery. Institutional review board approval and patient informed consent were obtained. The patient received a custom tibial prosthesis instrumented with four uniaxial force transducers, a microtransmitter, and an antenna.

Implant alignment was assessed radiographically. The angle between the bottom surface of the tibial tray and the tibial shaft (i.e., a line through the midpoint of the tibial cut and the center of the talus) was 90.1°. The target was 90° and the measurement error was approximately 0.5°. The femoral component was aligned at 6° valgus to the anatomic axis of the femur. The mechanical axis of the lower limb (center of femoral head to center of ankle) passed through a point 5% lateral to the midpoint of the tibial tray.

In vivo tibial force data were recorded simultaneously with fluoroscopic motion analysis data during treadmill gait (hands resting on handlebars), step up/down, kneel, and lunge activities.[17–20] The fluoroscopic and tibial force data were collected at different sampling frequencies using different data collection systems that did not possess a common synchronizing signal. All data were resampled at a common frequency during postprocessing. Additional overground gait trials were performed during which the instrumented implant data collection system also recorded the vertical ground reaction force signals from two force plates.

Following data collection, the fluoroscopic and tibial force data were synchronized to define motion cycles for subsequent data analysis. For gait, the cycle was defined to begin at right heel strike. From the overground gait data, we identified an inflection in the tibial force curve at the point where the vertical ground reaction force transitioned from zero to nonzero. The same inflection point in the tibial force data was used to identify right heel strike during treadmill gait. The start and end of the gait cycle in the fluoroscopic data were identified by the lowest point in the knee flexion curve. For step up/down, the cycle started when the tibial force began to rise and ended when it returned to its starting value. Maximum knee flexion was used to identify the start and end of the same cycle for the fluoroscopic data. For kneel and lunge, time frames were analyzed only from the final static pose, which was held by the patient for several seconds and possessed an approximately constant tibial load and knee flexion angle. These two activities were only partially weight bearing because the patient was standing on the opposite leg.

To facilitate subsequent contact analyses, one set of kinematic and tibial force data were constructed from the synchronized experimental data for each activity. For gait, horizontal knee translations combined with fluoroscopic field of view limitations necessitated the use of two fluoroscope positions to image the entire cycle.[17,20] Consequently, we created a single composite gait cycle by averaging eight cycles of fluoroscopic data (four from each half of the gait cycle) and 12 cycles of tibial force data including the same time frames. Different numbers of cycles were averaged to make use of all data available for analysis. For step up/down, no data averaging was required because a complete motion cycle was visible fluoroscopically. Hence, a single representative step up/down cycle was selected for analysis. For kneel and lunge, joint pose at the most highly flexed position was determined by averaging five and nine, respectively, time frames of fluoroscopic data. Different numbers of time frames were averaged to make use of all data available at the final static pose. Approximately constant tibial force data spanning the same time frames were identified, and the mean, minimum, and maximum force and corresponding center of pressure measurements were used in the subsequent analyses. The duration of the resulting cycles was 1.11 s for gait and 3.20 s for step up/down.

For the treadmill gait data, two additional steps were taken to synchronize fluoroscopic and instrumented implant data on an objective basis. First, because the averaging process caused slight inconsistencies, we phase shifted the kinematic data slightly forward and backward in time to find the position (2% of the cycle forward) that minimized root-mean-square (RMS) errors in predicted anterior-posterior (AP) center of pressure (CoP). Second, because the fluoroscopic measurements possessed error as well, we offset the AP translation at each time point within the range of ± 1 mm, the error bound on the experimental measurement.[17] The offset for each point was selected so as to minimize the AP CoP error at that time instant. Similar steps were not taken for the medial-lateral (ML) CoP because the contact model was allowed to equilibrate in the ML direction under the action of the applied loads. This approach made the data synchronization process for treadmill gait objective without markedly influencing the results.

Dynamic contact models (i.e., multiple time frames of gait and step up/down) and static contact models (i.e., a single time frame of kneel and lunge) of the patient's knee implant were constructed to predict in vivo contact forces on the medial and lateral contact surfaces of the tibial insert. The models were implemented within the Pro/MECHANICA MOTION simulation environment (PTC, Waltham, MA) (Fig. 1). A six degree-of-freedom (DOF)

 DOI 10.1002/jor

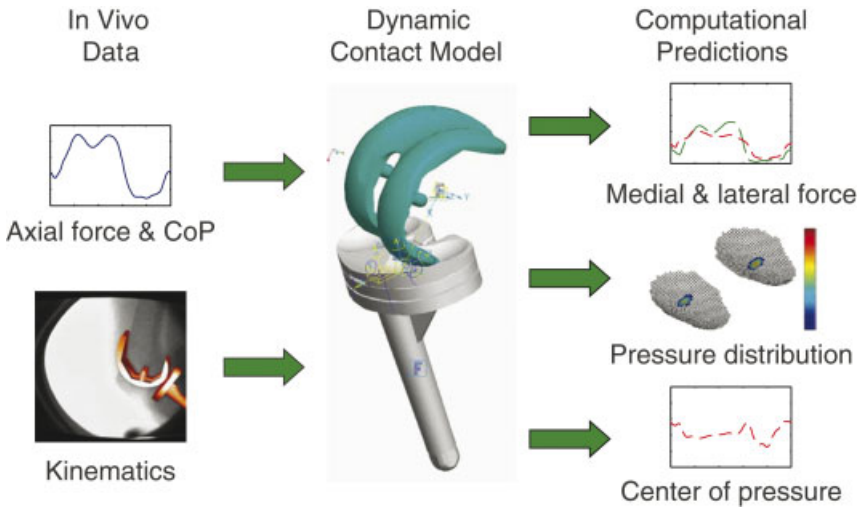

Figure 1. Overview of the experimental and computational methods used to develop and evaluate the dynamic contact model of the instrumented knee implant. In vivo fluoroscopic motion and telemetric force measurements provide accurate kinematic and force inputs to a dynamic contact model. The model predicts medial and lateral contact force, distributed contact pressure, and center of pressure (CoP) over a motion cycle. The predictions are evaluated by comparing measured and predicted CoP locations. [Color scheme can be viewed in the online issue, which is available at http://www.interscience.wiley.com]

joint between the femoral component and tibial insert was used to measure relative (i.e., joint) kinematics for contact calculations. The experimentally measured tibial force was applied to the back side of the tibial tray at the experimentally measured CoP location. Consequently, the femoral component was fixed to ground and the tibial component allowed to move relative to it. AP translation, internal-external rotation, and flexion-extension were prescribed to match the fluoroscopically measured kinematics while the other three DOFs were predicted via forward dynamic simulation or static analysis.[15]

A custom deformable contact model based on elastic foundation theory[15,21–24] was incorporated into the Pro/MECHANICA MOTION models using the custom load interface. The contact model utilized springs distributed uniformly over the articulating surfaces of the tibial insert to prevent excessive interpenetration, where each spring was associated with a single tibial surface element of known area. The contact pressure p for each element was calculated from

$$p = \frac{(1-\nu)E(p)}{(1+\nu)(1-2\nu)}\frac{d}{h} \tag{1}$$

where $E(p)$ is Young's modulus of the elastic layer (constant for the linear material and a function of p for the nonlinear material[31]), ν is Poisson's ratio of the elastic layer, h is the layer thickness at the element location, and d is the element's spring deflection, defined as the interpenetration of the undeformed surfaces in the direction of the local surface normal. d was computed at each time instant given the relative position and orientation of the insert with respect to the femoral component as obtained from the six DOF joint in the Pro/MECHANICA MOTION model. The three-dimensional contact force vector acting on each side of the insert was computed by multiplying the element pressures by their respective areas and performing a vector summation over all elements. Medial and lateral contact forces were calculated by taking the axial components of the two contact force vectors. Evaluation of the calculated contact forces was performed by comparing measured and predicted CoP locations for the entire tibial insert in the ML and AP directions.

Element contact pressures were calculated using linear and nonlinear material models with a Poisson's ratio of 0.46.[25] Two material models were used to determine the sensitivity of predicted medial-lateral contact forces to the choice of model. For the linear model, Young's modulus was set to 463 MPa for all elements.[30] For the nonlinear model the modulus was set to a different value for each element depending on its current level of contact pressure. The relationship between modulus and contact pressure was derived from a modified nonlinear power law[23]:

$$\varepsilon = \frac{1}{2}\varepsilon_o\frac{p}{p_o} + \frac{1}{2}\varepsilon_o\left(\frac{p}{p_o}\right)^n \tag{2}$$

where ε is element strain and ε_o, p_o, and n are material parameters. Values for these parameters were set to $\varepsilon_o = 0.0257$, $p_o = 15.9$ MPa, and $n = 3$ based on fitting of

experimental stress-strain data for polyethylene.[26] The initial modulus of the nonlinear model (1237.4 MPa) was greater than that of the linear model. For any specified value of element pressure, $E = dp/d\varepsilon$ was calculated from Equation 2 as

$$E(p) = 1/\left\{\frac{1}{2}\frac{\varepsilon_o}{p_o}\left[1 + n\left(\frac{p}{p_o}\right)^{n-1}\right]\right\} \quad (3)$$

Equation 3 was then substituted into Equation 1 to produce a single nonlinear equation with p as the only unknown. During a simulation, Equation 3 was solved for each element using a nonlinear rootfinding algorithm. Further details for performing dynamic and static contact analyses using multibody simulation methods can be found in reference 27.

RESULTS

The ratio of medial to total contact force as calculated by the contact model varied between and within activities (Fig. 2). Despite differences in predicted contact pressures (Fig. 3), predicted contact forces were insensitive to choice of material model. Medial contact force followed the trend of total contact force better than did lateral contact force for both gait and step up/down (Fig. 2, top and middle). Step up/down exhibited the largest medial and lateral contact forces, followed by gait, lunge, and kneel. At maximum load, medial force was 2.0 BW for step up/down and 1.2 BW for gait, while the corresponding lateral forces were 1.5 and 1.0 BW, respectively (Table 1). At mean load in the final static pose, medial force was 0.2 BW for kneel and 0.9 BW for lunge, with corresponding lateral forces of 0.1 and 0.7 BW, respectively (Table 1). The ratio of medial to total force (reported as a percentage) ranged from 18 to 60% for the entire gait cycle, averaging 55% during midstance phase and 33% during swing phase, and from 47 to 65% for the entire step up/down cycle (Fig. 2, bottom). The ratio was much more constant for step up/down than for gait over a single cycle. At maximum load, the ratio was between 53 and 60% for all four activities (Table 1).

Predicted CoP locations matched the experimental measurements over most of the gait cycle and the entire step up/down cycle. Similar to contact forces, results from the two material models were nearly identical. Without changing any fluoroscopically measured motion inputs, the contact simulations reproduced the ML location of the CoP very closely for all activities with RMS errors of 0.6 mm for gait and 0.0 mm for step up/down, kneel, and lunge. In contrast, the simulations matched the AP location of the CoP well only for the stance phase of gait and for step up/down, with RMS errors of 4.8 mm over the entire gait cycle, 1.9 mm during stance phase, and 1.3 mm for step up/down. When the fluoroscopically measured AP translations were adjusted within their range of experimental error (±1 mm), RMS errors in the AP CoP location were reduced to 3.5 mm over the entire gait cycle, 0.5 mm during stance phase, and 0.5 mm for step up/down (Fig. 2). At maximum load for each

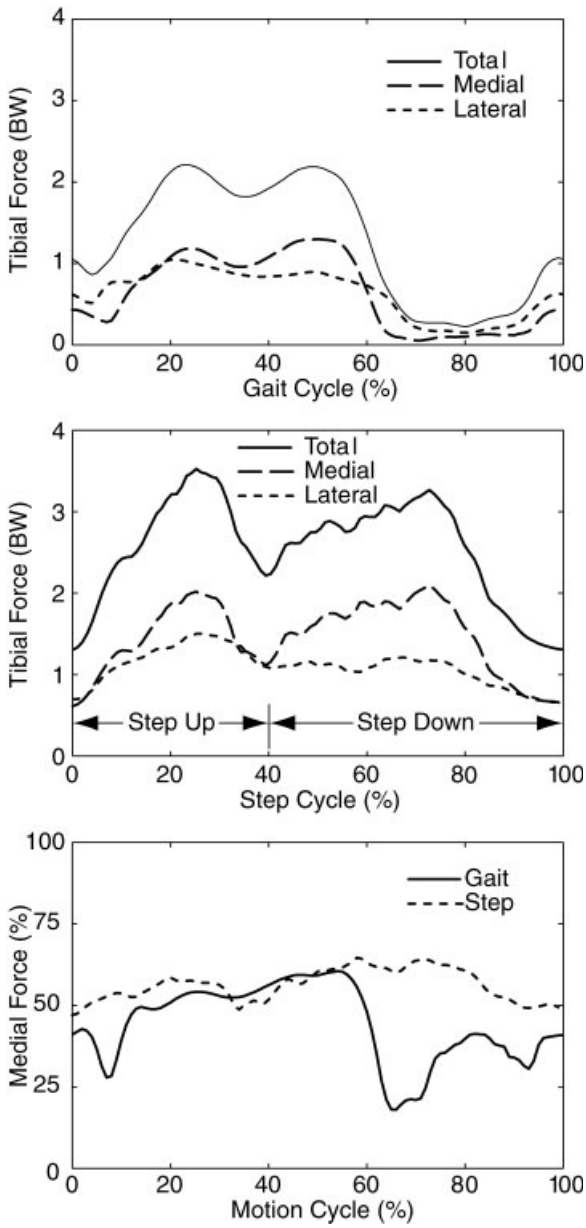

Figure 2. Medial and lateral contact forces calculated during gait (top) and step up/down (middle) activities and the percentage of medial-to-total contact force over the gait and step cycle (bottom). Results are plotted only for the linear material model because results for the nonlinear model were indistinguishable.

 DOI 10.1002/jor

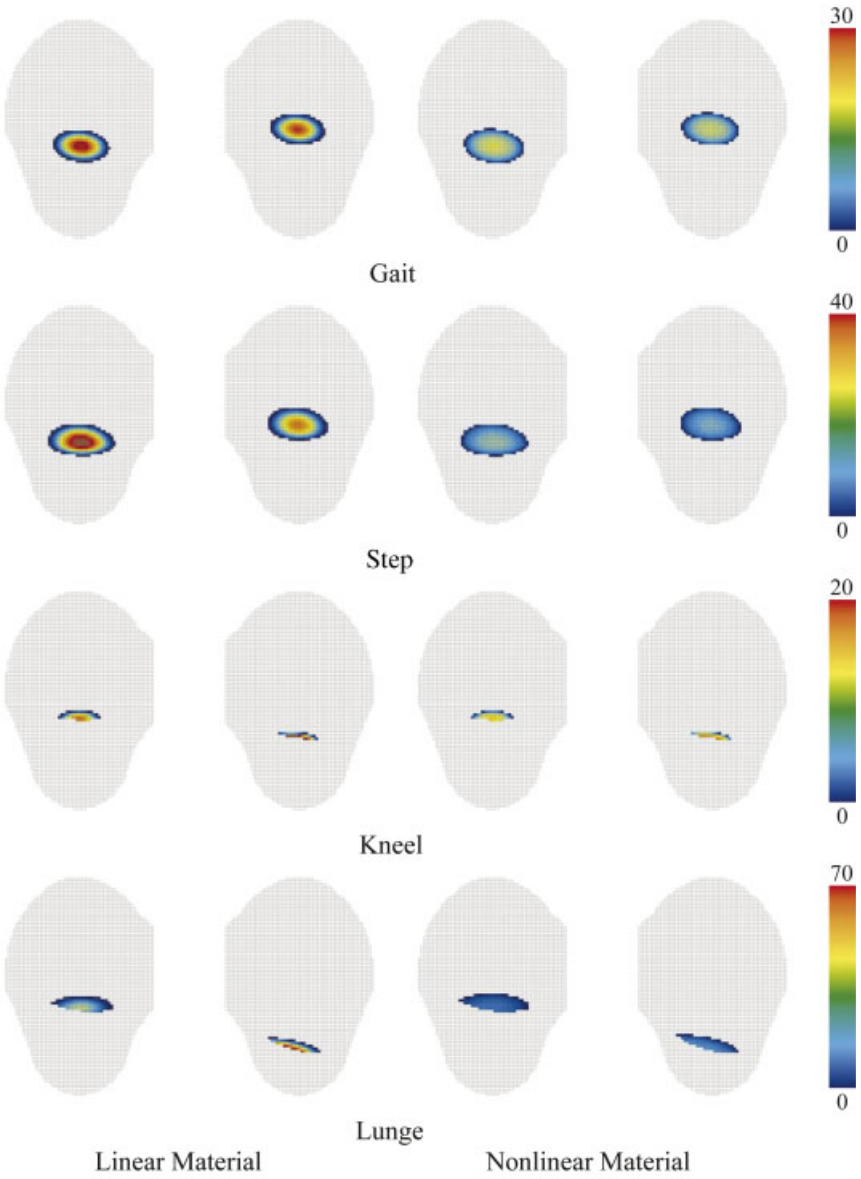

Figure 3. Visualization of contact pressures exerted on the tibial insert at maximum load during gait, step up/down, kneel, and lunge activities using linear and nonlinear material models. Maximum load does not necessarily correspond to maximum pressure due to the effect of contact geometry on the pressure calculations. [Color scheme can be viewed in the online issue, which is available at http://www.interscience.wiley.com]

Table 1. Medial-to-Total Force Percentage, Contact Force, and AP CoP Error for Gait, Step Up/Down, Lunge, and Kneel Activities Using the Linear Material Model

			Force (BW)		AP CoP Error (mm)	
Activity	Load (BW)	Medial/Total Force (%)	Medial	Lateral	Original	Adjusted
Gait	2.2	53.4	1.2	1.0	2.9	1.0
Step	3.5	56.0	2.0	1.5	0.3	0.2
Kneel	0.3 (0.2, 0.4)	57.0 (55.2, 59.6)	0.2 (0.1, 0.2)	0.1 (0.1, 0.2)	11.6 (12.6,11.2)	10.4 (11.5,10.1)
Lunge	1.6 (1.2, 2.2)	57.7 (56.6, 57.5)	0.9 (0.7, 1.3)	0.7 (0.5, 0.9)	2.9 (3.1, 1.2)	1.7 (2.0, 0.1)

For gait and step up/down, results are reported at maximum load. For kneel and lunge, results are reported for mean load with additional results for minimum and maximum load over the interval indicated in parentheses.

activity, CoP error in the AP direction was smallest for step up/down and largest for kneel, ranging from 0.2 to 11.5 mm after AP translation adjustment (Table 1).

DISCUSSION

This study used a novel combination of an instrumented knee implant, fluoroscopic motion analysis, and a deformable contact model to determine in vivo medial and lateral contact forces on the tibia during treadmill gait (hands resting on handlebars), step up/down, kneel, and lunge activities. Medial and lateral contact force calculations were insensitive to choice of material model (linear or nonlinear), with the ratio of medial to total contact force being close to 50% for high-loading phases of all activities. CoP calculations were also insensitive to choice of material model, and the reliability of the calculated medial and lateral contact forces was supported by the model's ability to reproduce the experimentally measured AP and ML CoP locations. Contact pressures predicted by the model followed the same trends as medial and lateral contact force for gait and step up/down. Though a constant load split of 55% medial–45% lateral would be a reasonable approximation for the current patient performing gait, step up/down, kneel, and lunge activities, the reasonableness of this approximation for the general patient population is unknown.

While previous studies reported that the majority of the load passes through the medial compartment during gait, our study found a more equal medial-lateral load split. To our knowledge, all previous estimates of medial-lateral load split during gait have been based on biomechanical models without internal load measurements.[4–9] Most estimates were derived from models that required prediction of individual muscle forces, and these predictions may have been sensitive to errors in muscle origin and insertion locations, moment arms, and peak isometric strength values. Furthermore, previous studies did not have a method for evaluating the reasonableness of the predicted medial-lateral load split. In our study, prediction of individual muscle forces was not needed due to the availability of internal force measurements, and the load split calculations could be evaluated using the experimentally measured CoP locations.

One possible explanation for the near-equal medial-lateral load split during gait was that the subject was allowed to rest his hands on the handlebars of the treadmill for balance and safety reasons. Even though the subject was extremely stable and in excellent condition, we wanted to minimize the possibility of him falling on the treadmill. Resting the hands on the treadmill handlebars had two effects. First, it provided the subject with some force feedback that may have improved his ability to balance. Second, the subject did not swing his arms during treadmill gait, in contrast to overground gait where arm swing occurs out of phase with leg swing. Consequently, at right heel strike on the treadmill, the right arm was forward instead of in its usual backward position, while at right toe off, the right arm was forward in a position similar to its usual forward position.

Given these issues, we assessed whether our treadmill results were indicative of overground gait by following a two-step process. First, we evaluated the accuracy with which medial contact force can be estimated directly from the two medial load cell measurements. The sum of the two medial load cell measurements need not equal the medial contact force calculated by the contact model (see Appendix). However, when we performed the comparison for the treadmill gait data, we found that the medial force curves calculated by the two approaches were nearly identical, with maximum and RMS differences of 0.03 and 0.01 BW, respectively. For the step up/down, kneel, and lunge data, the maximum error was 0.14 BW with an RMS difference of 0.04 BW for step up/down. Thus, while we could not prove ahead of time that the medial contact force is the sum of the two medial load cell measurements, our contact model calculations support this conclusion, at least for this instrumented implant design and activities without significant internal-external rotation (see Appendix for further discussion).

Based on this finding, we then used the load cell measurements directly to compare the total axial load and medial-lateral load split between treadmill and overground gait. The total axial load profiles were similar with an RMS difference of 0.15 BW. In contrast, the medial-lateral load split during overground gait was larger during midstance (i.e., about 15 to 45% of the cycle) but comparable at the start and end of stance. The maximum difference occurred at about 20% of the cycle, where 70% of the load passed through the medial compartment during overground gait but only 50% during treadmill gait. This finding is consistent with force feedback to the hands and altered arm positioning during this portion of the treadmill gait cycle. Thus, our treadmill gait measurements may have underestimated the

 DOI 10.1002/jor

amount of load passing through the medial compartment during midstance of overground gait.

We also assessed the reasonableness of our computational procedure by evaluating whether inaccurate model prediction of varus-valgus (VV) rotation or ML translation would lead to inaccurate prediction of the CoP. To mimic a rigid body analysis, we performed static analyses for the initial time frame of gait but with ML translation or VV rotation locked to specific values rather than left free. ML translation was varied by ± 1 mm about its nominal position, whereas VV rotation was varied by $\pm 0.1^{\circ}$. These small variations changed the predicted ML CoP by about 25 mm. Because single plane fluoroscopy can measure ML translation to within about 6.6 mm and VV rotation to within about 1°,[17] using the fluoroscopically measured kinematics directly for these two DOFs would not produce ML CoP and contact force predictions consistent with the experimental data. The model's predictions for these two DOF were within the confidence limits of their fluoroscopically measured motions, supporting the reasonableness of this approach.

Errors in the predicted CoP locations were small apart from the AP direction during the swing phase of gait and during kneel (Fig. 4). The CoP locations measured by the instrumented implant have been shown to be accurate to within ± 2 mm for loads ranging from 800 to 2,000 N.[10] Maximum errors in predicted CoP location were about 10 mm in the AP direction for loads in the range of 150 N (swing phase of gait) to 200 N (kneel). Because the experimental CoP calculation involves dividing by the total axial load, the calculation will be most sensitive to axial load measurement errors when the load is "small." Consequently, when we plotted AP CoP error as a function of the inverse of the axial load, we found a high correlation ($R^2 = 0.80$, Fig. 5). Thus, sensitivity of the experimental CoP calculations to errors in the measured axial load helps explain the large AP CoP errors during light loading. Data averaging may have also contributed to AP CoP errors, consistent with the observation

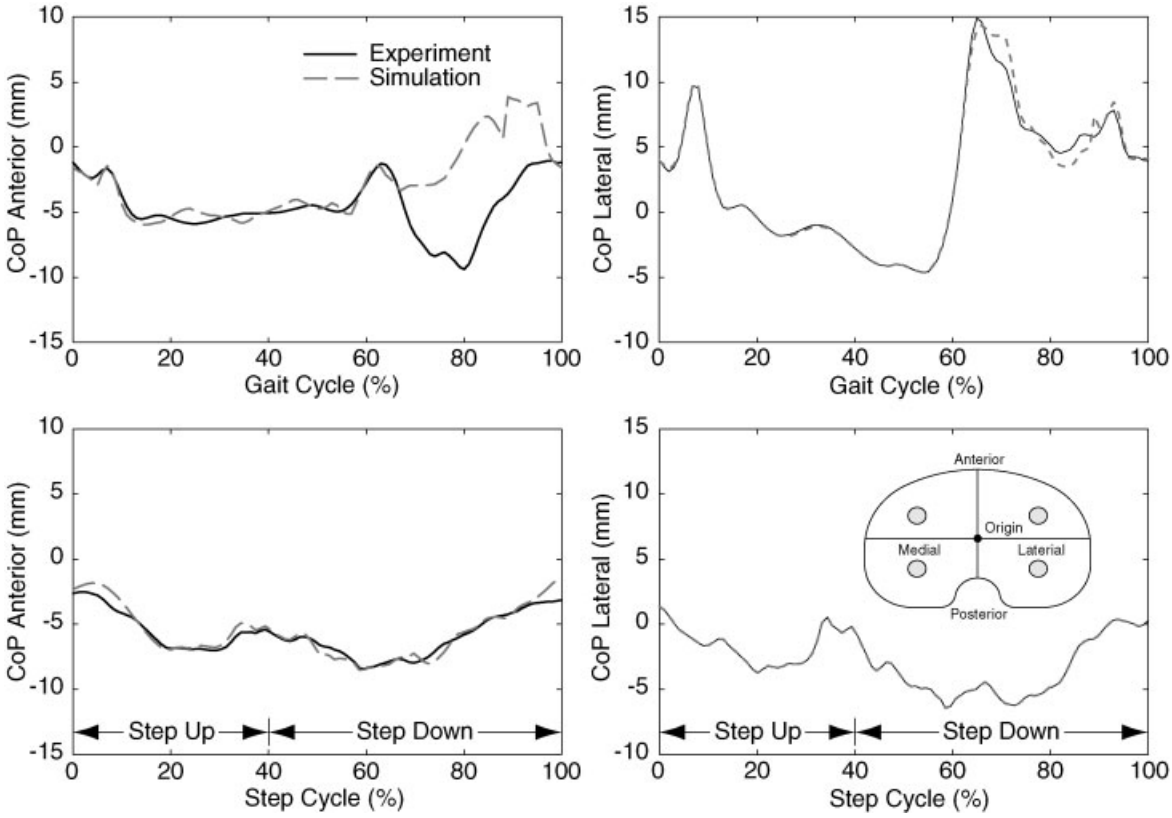

Figure 4. Comparison of experimental and simulated center of pressure locations in the AP (anterior is positive) and ML (lateral is positive) directions for gait (top row) and step up/down (bottom row) activities. Results are plotted only for the linear material model because results for the nonlinear model were indistinguishable. The coordinate system origin of the tibial insert, located at the geometric center of the back surface, is the zero reference point for AP and ML translations (see inset in lower right plot).

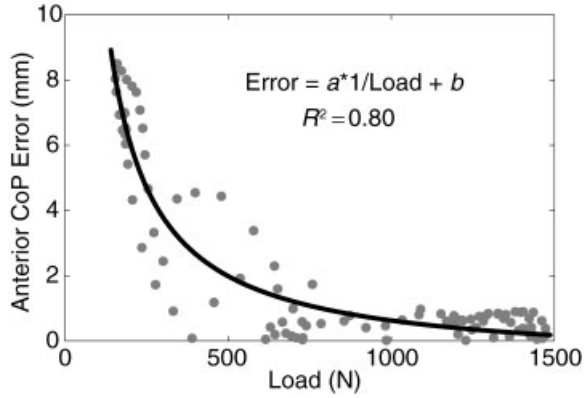

Figure 5. Error in predicted AP center of pressure location as a function of the inverse of the applied axial load during gait.

that the unaveraged step up/down data set had the lowest errors. Because researchers are most interested in phases of high rather than low loading, CoP errors during light loading periods are not a critical limitation of the study.

The primary limitation of this study is that only a single patient with an implanted knee could be analyzed. This limitation is due to the difficulty of obtaining the in vivo experimental measurements of implant motions and loads required as inputs to the contact model. Although the patient's walking speed (1.24 ± 0.03 m/s) and ground reaction forces were similar to those of normal subjects,[28,29] we are still limited by the use of only a single subject. The extent to which these results apply to knee implant patients in general or to nonimplanted knees is unknown.

The kneel and lunge tests were included to investigate static loads in deep flexion positions. They provide no information on the dynamic loads that occurred while reaching the final static pose. Furthermore, these static poses may not be representative of deep flexion poses that occur during normal daily activities. Nonetheless, these poses were worth studying because sustained deep flexion occurs in daily life in some cultures. Understanding internal medial and lateral contact loads under such static conditions could be helpful for designing total knee replacements that function well in deep flexion.

In summary, this study presented a novel approach of combining in vivo load and motion measurements with a computational model to predict the medial-lateral force distribution in an implanted knee during a variety of activities. The in vivo medial-to-total force ratio and contact pressure results may be valuable for improving our understanding of knee joint mechanics and developing computational and experimental testing protocols to assess wear performance of new knee implant designs. However, the extent to which our results apply to nonlaboratory conditions is unknown.

ACKNOWLEDGMENTS

This work was supported by an NSF CAREER award to B.J. Fregly, the Biomotion Foundation of Palm Beach, FL, and Shiley Center for Orthopaedic Research & Education at Scripps Clinic, La Jolla, CA.

APPENDIX

In this Appendix, we investigate the question of whether the sum of the two medial load cell measurements should equal the medial contact force. To answer this question, consider Figure A1 (A1), which shows a coronal view of the loading situation on the instrumented implant. In this schematic, *FM* is the total uniaxial load measured by the two medial load cells, *FL* the total uniaxial load measured by the two lateral load cells, *AM* the medial contact force, *AL* the lateral contact force, d the fixed distance from the center of the tibial tray to the medial and lateral load cells, and a and b the variable distances to the medial and lateral contact loads, respectively.

Engineering statics can be used to solve for *AM* and *AL* as a function of *FM*, *FL*, a, b, and d. Summing forces in the vertical direction yields

$$AM + AL + FM + FL \qquad \text{(A1)}$$

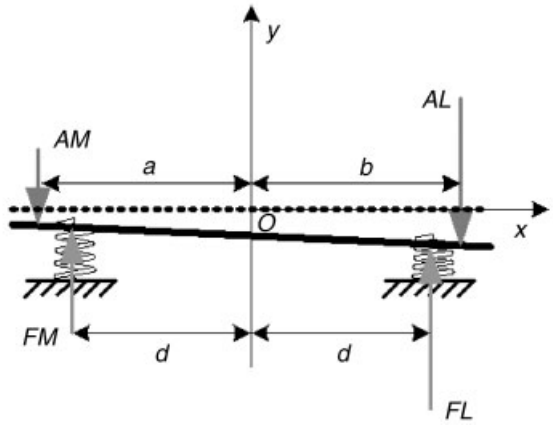

Figure A1. Schematic representation of the medial-lateral loading situation for the instrumented implant.

 DOI 10.1002/jor

while summing moments about the center point O produces

$$a\,AM - b\,AL = d(FM - FL) \qquad \text{(A2)}$$

Because a and b are unknown, we have two equations in four unknowns. Consequently, we will solve Equations A1 and A2 for AM and AL assuming the values of a and b are known:

$$\begin{aligned} AM &= \tfrac{b+d}{a+b}FM + \tfrac{b-d}{a+b}FL \\ AL &= \tfrac{a-d}{a+b}FM + \tfrac{a+d}{a+b}FL \end{aligned} \qquad \text{(A3)}$$

From Equation A3, it is clear that we will obtain $AM = FM$ and $AL = FL$ if and only if $a = d$ and $b = d$. In other words, the sum of the two medial load cell measurements will equal the medial contact force only if the CoP *on each side* is directly over the two load cells on that side in the AP direction.

When we calculated the CoP *on each side* using our contact model, we found that the data approximately satisfied these requirements. During treadmill gait for example, the medial CoP location (i.e., a in Fig. A1) varied between -22.2 and -17.0 mm and the lateral CoP location (i.e., b in Fig. A1) varied between 18.9 and 22.7 mm. The medial-lateral distance from the center line of the tibial tray to each load cell (i.e., d in Fig. A1) was 20.4 mm. If the medial-lateral spacing between the femoral condyles or between the load cells had been different, approximating the medial contact force with the sum of the two medial load cell measurements would have been less reasonable. It is also possible that other activities not measured in our study could produce larger axial rotations or medial-lateral translations that would make this approximation less accurate.

REFERENCES

1. Jackson BD, Wluka AE, Teichtahl AJ, et al. 2004. Reviewing knee osteoarthritis—a biomechanical perspective. J Sci Med Sport 7:347–357.
2. Andriacchi TP, Stanwyck TS, Galante JO. 1986. Knee biomechanics and total knee replacement. J Arthroplasty 1:211–219.
3. Morrison JB. 1970. The mechanics in knee joint in relation to normal walking. J Biomech 3:51–61.
4. Hsu RW, Himeno S, Coventry MB, et al. 1990. Normal axial alignment of the lower extremity and load-bearing distribution at the knee. Clin Orthop 255:215–227.
5. Hurwitz DE, Sumer DR, Andriacchi TP, et al. 1998. Dynamic knee loads during gait predict proximal tibial bone distribution. J Biomech 31:423–430.
6. Johnson F, Leitl S, Waugh W. 1980. The distribution of load across the knee: A comparison of static and dynamic measurements. J Bone Joint Surg 62B:346–349.
7. Noyes FR, Schipplein OD, Andriacchi TP, et al. 1992. The anterior cruciate ligament-deficient knee with varus alignment. An analysis of gait adaptations and dynamic joint loadings. Am J Sports Med 20:707–716.
8. Shelburne KB, Torry MR, Pandy MG. 2005. Muscle, ligament, and joint-contact forces at the knee during walking. Med Sci Sports Exerc 37:1948–1956.
9. Schipplein OD, Andriacchi TP. 1991. Interaction between active and passive knee stabilizers during level walking. J Orthop Res 9:113–119.
10. D'Lima DD, Townsend CP, Arms SW, et al. 2005. An implantable telemetry device to measure intra-articular tibial forces. J Biomech 38:299–304.
11. Taylor SJ, Perry JS, Meswania JM, et al. 1997. Telemetry of forces from proximal femoral replacements and relevance to fixation. J Biomech 30:225–234.
12. Taylor SJ, Walker PS, Perry JS, et al. 1998. The forces in the distal femur and the knee during walking and other activities measured by telemetry. J Arthroplasty 13:428–437.
13. Blunn GW, Walker PS, Joshi A, et al. 1991. The dominance of cyclic sliding in producing wear in total knee replacements. Clin Orthop Relat Res 273:253–260.
14. DesJardins JD, Walker PS, Haider H, et al. 2000. The use of a force-controlled dynamic knee simulator to quantify the mechanical performance of total knee replacement designs during functional activity. J Biomech 28:1231–1242.
15. Fregly BJ, Sawyer WG, Harman MK, et al. 2005. Computational wear prediction of a total knee replacement from in vivo kinematics. J Biomech 38:305–314.
16. Périé D, Hobatho MC. 1998. In vivo determination of contact areas and pressure of the femorotibial joint using non-linear finite element analysis. Clin Biomech (Bristol, Avon) 13:394–402.
17. Banks SA, Hodge WA. 1996. Accurate measurement of three-dimensional knee replacement kinematics using single-plane fluoroscopy. IEEE Trans Biomed Eng 43: 638–649.
18. Banks SA, Markovich GD, Hodge WA. 1997. In vivo kinematics of cruciate-retaining and substituting knee arthroplasties. J Arthroplasty 12:297–304.
19. Banks SA, Markovich GD, Hodge WA. 1997. The mechanics of knee replacements during gait: in vivo fluoroscopic analysis of two designs. Am J Knee Surg 10: 261–267.
20. Dennis DA, Komistek RD, Mahfouz MR. 2003. In vivo fluoroscopic analysis of fixed-bearing total knee replacements. Clin Orthop Relat Res 410:114–130.
21. An KN, Himeno S, Tsumura H, et al. 1990. Pressure distribution on articular surfaces: application to joint stability evaluation. J Biomech 23:1013–1020.
22. Blankevoort L, Kuiper JH, Huiskes R, et al. 1991. Articular contact in a three-dimensional model of the knee. J Biomech 24:1019–1031.
23. Fregly BJ, Bei Y, Sylvester ME. 2003. Experimental evaluation of anelastic foundation model to predict contact pressures in knee replacements. J Biomech 36:1658–1668.
24. Johnson KL. 1985. Contact Mechanics. Cambridge: Cambridge University Press.
25. Bartel DL, Rawlinson JJ, Burstein AH, et al. 1995. Stresses in polyethylene components of contemporary total knee replacements. Clin Orthop Relat Res 317:76–82.

26. Cripton PA. 1993. Compressive characterization of ultra-high molecular weight polyethylene with applications to contact stress analysis of total knee replacements. Master of Science Thesis. Queen's University, Kingston, Ontario.
27. Bei Y, Fregly BJ. 2004. Multibody dynamic simulation of knee contact mechanics. Med Eng Phys 26:777–789.
28. Andriacchi TP, Galante JO, Fermier RW. 1982. The influence of total knee-replacement design on walking and stair-climbing. J Bone Joint Surg Am 64:1328–1335.
29. Chao EY, Laughman RK, Schneider E, et al. 1983. Normative data of knee joint motion and ground reaction forces in adult level walking. J Biomech 16:219–233.
30. Kurtz SM, Jewett CW, Bergstrom JS, et al. 2002. M iniature specimen shear punch test for UHMWPE used in total joint replacements. Biomaterials 23:1907–1919.
31. Nuño N, Ahmed AM. 2001. Sagittal profile of the femoral condyles and its application to femorotibial contact analysis. J Biomech Eng 123:18–26.

 DOI 10.1002/jor